Am J Cancer Res 2026;16(9):4152-4169
www.ajcr.us /ISSN:2156-6976/ajcr0174577

Original Article

MKRN2 promotes gastric cancer progression by suppressing autophagy via the PI3K/Akt/mTOR signaling pathway

Miao Wang, Nan Hou, Honglei Wang, Xuqing Ding, Xinchao Sun, Junjie Tu

Department of Oncology, Nanyang Second General Hospital, Nanyang 473000, Henan, China

Received June 8, 2026; Accepted September 23, 2026; Epub September 25, 2026; Published September 30, 2026

Abstract: Makorin ring finger protein 2 (MKRN2) is associated with the development of various tumors; however, few studies have investigated the role MKRN2 in gastric cancer (GC). This study aimed to investigate the expression and underlying mechanism of MKRN2 in GC. Quantitative real-time PCR (qRT-PCR) and western blotting were adopted to detect MKRN2 expression in GC cells. Cell viability, colony formation, and apoptosis were determined using cell counting kit-8 (CCK-8) assay, colony formation assay, and terminal deoxynucleotidyl transferase dUTP nick end labeling (TUNEL) assay, respectively. Cell invasion and migration were evaluated using transwell and scratch healing assays. Flow cytometry and immunofluorescence were performed to evaluate M1/M2 macrophage phenotypes. Western blotting was adopted to measure the expression of autophagy-related proteins and components of the phosphatidylinositol 3-kinase/protein kinase B/mammalian target of rapamycin (PI3K/Akt/mTOR) pathway. An *in vivo* xenograft mouse model was established by subcutaneous injection of MKN-45 cells. The expression Ki-67 and MKRN2 in GC tissues was detected by immunohistochemistry (IHC). MKRN2 expression was elevated in GC. MKRN2 overexpression promoted cell proliferation, migration and invasion, whereas MKRN2 knockdown inhibited those cellular behaviors. MKRN2 knockdown increased LC3-II/LC3-I ratio and Beclin1 expression, and decreased p62 level, whereas MKRN2 overexpression produced the opposite effects. Treatment with 3-methyladenine (3-MA) partly reversed autophagy-related changes in GC cells induced by MKRN2 knockdown. On contrary, rapamycin (RAPA) treatment counteracted the inhibition of autophagy caused by MKRN2 overexpression. MKRN2 knockdown reduced xenograft tumor growth in mice. Moreover, MKRN2 knockdown inhibited the phosphorylation and activation of the PI3K/Akt/mTOR pathway. MKRN2 knockdown inhibited M2 macrophage polarization and promoted M1 macrophage polarization. MKRN2 may partook in the pathogenesis and development of GC as an oncogene. These findings laid a foundation for the development of targeted therapy in GC progression.

Keywords: Makorin ring finger protein 2, gastric cancer, malignant progression, M2 macrophage, phosphatidylinositol 3-kinase/protein kinase B/mammalian target of rapamycin pathway

Introduction

Gastric cancer (GC) is one of the common gastrointestinal malignancies worldwide. In 2022, an estimated 968,000 new cases of GC and 660,000 GC-related deaths occurred globally [1]. Because early-stage GC often presents with nonspecific symptoms and the current screening rates remain low, many patients are not diagnosed until an advanced stage, greatly limiting the opportunity for surgical intervention. Therefore, effective nonsurgical treatments are required to prolong survival and improve the quality of life of patients with GC. Current non-surgical treatment strategies for GC primarily include chemotherapy [2], radiotherapy, molecular targeted therapy, immunotherapy, or combination therapy. Despite recent advances, the overall prognosis of GC patients remains unsatisfactory [3-5]. The onset of GC The onset of GC is influenced by multiple factors, and its occurrence and progression involve a series of complex molecular events [6]. However, the underlying molecular mechanisms have not yet been fully elucidated, posing challenges to the treatment and prognostic management of GC. Therefore, identifying novel therapeutic approaches, targets, and strate-

https://doi.org/10.62347/VCYR1308

gies, os of significant clinical importance for the treatment of GC.

Makorin ring finger protein 2 (MKRN2) belongs to the MKRN gene family and is presumed to have originated from an ancestral MKRN1 gene through gene duplication approximately 450 million years ago [7]. Other family members, including MKRN3 and MKRN4, have also been implicated in various diseases. In mammals, the nucleotide sequence of MKRN2 partially overlaps with another gene in an antisense transcriptional orientation [8], suggesting potential regulatory interactions between these genetic elements. MKRN2 is a zinc finger protein with a characteristic C3HC4 protein-protein interaction motif (known as the RING domain) and belongs to the E3 ubiquitin ligase family. E3 ubiquitin ligases are essential enzymes that mediates the transfer of ubiquitin from E2 ubiquitin-conjugating enzymes to specific protein substrates [9]. Existing evidence indicates that MKRN2 is involved not only in inflammation, diabetes wound healing, lumbar spinal stenosis, male reproductive dysfunction, and other disease processes [10-12], but also in the tumorigenesis of various malignancies [13-15]. MKRN2 is upregulated in hepatocellular carcinoma and promotes cell-cycle progression and proliferation [16]. Conversely, MKRN2 has exhibited tumor-suppressive effects in other malignancies. It attenuates the progression of clear cell renal cell carcinoma via regulating the protein phosphatase 2 catalytic subunit alpha (PPP2CA)/β-catenin/Wnt pathway [17], and inhibits neuroblastoma cell proliferation and migration [18]. Liu et al. also found that MKRN2 notably inhibited cell proliferation by promoting the degradation of pyruvate kinase M2 (PKM2) [19].

The tumor microenvironment (TME) is a complex and continuously evolving ecosystem comprising tumor cells, non-tumor cellular components, and their related metabolites within a specific spatial environment [20]. Studies of the TME have demonstrated that specific immune cell populations, including tumor associated macrophages (TAMs), myeloid derived inhibitory cells (MDSCs), and regulatory T cells (Tregs), play central immunosuppressive roles in regulating antitumor immune responses [21]. TAMs represent one of the predominant immune cell populations infiltrating the TME and are usually classified into M1-like macrophages (promoting anti-tumor immune response) and M2-like macrophages (fostering a tumor immunosuppressive microenvironment) [22]. A previous study reported a significantly accelerated growth of ID8 ovarian tumors in MKRN2 knockout mice, accompanied by significant alterations in macrophage phenotypes compared with those in wild-type controls. Specifically, MKRN2 deficiency inhibited the transition of TAMs from an antitumor M1 phenotype to a protumor M2 phenotype [13]. Although MKRN2 has been associated with the development of various cancers, its role in GC remains poorly understood, especially regarding its relationship with the TME and the underlying molecular mechanisms.

This study assessed MKRN2 expression in GC and investigated its functional role and underlying mechanisms in GC development. By establishing MKRN2 overexpression and knockdown cell models and conducting cellular functional assays and animal experiments, we systematically evaluated the regulatory effect of MKRN2 on GC progression and its effects on autophagy, macrophage polarization, and the PI3K/Akt/mTOR signaling pathway. This study provides an experimental basis and new ideas for the future development of MKRN2-targeted therapeutic strategies for GC.

Material and methods

Tissue collection

Forty-four patients with GC admitted to Nanyang Second General Hospital were enrolled in this study. GC tissues and corresponding adjacent normal tissues were collected. All sampling procedures and experimental protocols were approved by the Human Ethics Committee of Nanyang Second General Hospital (Approval ID: 2021-LY017-01-K01), and written informed consent was obtained from all patients. All tissue samples were stored at -80°C until further analysis.

Bioinformatics analysis

The Tumor Immune Estimation Resource (TIMER) 2.0 database (https://cistrome.shinyapps.io/timer/) was used to generate box plots showing MKRN2 expression in various malignancies. For differential expression analysis, tumor sam-

ples were ranked by MKRN2 expression and divided into MKRN2-low and MKRN2-high groups according to the median expression value as the cutoff. The University of Alabama at Birmingham Cancer data analysis Portal (UALCAN) database (https://ualcan.path.uab.edu/cgi-bin/ualcan-res.pl) was used to compare MKRN2 expression between normal and tumor tissues and to evaluate its associations with the clinicopathological features of GC patients.

Cell culture and transfection

MKN-7, MKN-45, AGS, HGC-27, THP-1, and the normal human gastric epithelial GES-1 cells were purchased from Wuhan Procell Life Technology Co., Ltd. All cell lines were authenticated by short tandem repeat (STR) testing, and mycoplasma testing was performed to exclude contamination. All cells were cultured in Roswell Park Memorial Institute (RPMI) 1640 medium (BIOAGRIO, Shanghai, China) supplemented with 10% fetal bovine serum (FBS; Thermo Fisher Scientific, Waltham, MA, USA) and 1% penicillin-streptomycin. Short hairpin RNA targeting MKRN2 (sh-MKRN2) and a negative control (sh-NC), as well as an MKRN2 overexpression plasmid (oe-MKRN2) and its corresponding negative control (oe-NC) were obtained from GenePharma. Transfection was performed using Lipofectamine 2000 (1166-8019; Thermo, Waltham, MA, USA) according to the manufacturer's instructions. Transfection efficiency was evaluated 48 h after transfection.

The shRNA sequences were as follows: Sh-NC, 5'-GCGCGATAGCGCTAATAATTT-3'; Sh-MKRN2#1, 5'-GACCTCTTCATGCACCTTTCT-3'; and Sh-MKRN2#2, 5'-GTCCAGAATGCCGTGTGATAT-3'.

Cell counting kit-8 (CCK-8)

Briefly, 5 × 10^3 cells GC cells with MKRN2 knockdown or overexpression were seeded into each well of a 96-well plate and subsequently cultured for 0, 24, 48, and 72 h. CCK-8 solution (Dojindo Molecular Technologies, Inc., Kumamoto, Japan) was then added, and the cells were incubated for an additional 2 h. Cell viability was subsequently measured using a microplate reader.

Colony formation assay

GC cells were inoculated into 6-well plates and cultured under standard conditions for 2-3 weeks. After two weeks, the cells were fixed with methanol and then stained. The plates were then washed and dried, and images were captured for calculating the number of colonies or the colony formation rate.

Terminal deoxynucleotidyl transferase dUTP nick end labeling (TUNEL)

GC cells were fixed with 4% paraformaldehyde, followed by rinsing with phosphate buffer saline (PBS) for 15 minutes. Subsequently, the cells were double-stained with a TUNEL staining reagent and 4'-6-diamidino-2-phenylindole (DAPI; Beyotime, Shanghai, China). Images were acquired using a fluorescent microscope (Olympus, Tokyo, Japan) at ×400 magnification.

Wound-healing assay

A straight wound was created across the cell monolayer using a sterile 200-μL pipette tip. The GC cells were washed and incubated in 2 mL of serum-free medium. Images were acquired using a microscope (CX23, Olympus) at a magnification of ×100 immediately after wounding and again after 48 h. The wound healing rate was calculated based on the change in wound area.

Transwell assay

GC cells (5 × 10^4 cells) were seeded into the upper compartment of a Transwell chamber (pore size, 8 μm) (Nest) that precoated with Matrigel. A total of 600 μL of culture medium was added to the lower chamber as a chemoattractant. Following incubation, the invaded cells were fixed with 4% paraformaldehyde, stained with 1% crystal violet, and observed under a light microscope.

Quantitative real-time PCR (qRT-PCR)

Total RNA was extracted from cells and tissue specimens using Trizol reagent (Beyotime-Scientific, China). cDNA was synthesized using RNA as the template, followed by RT-qPCR using a SYBR Green-based PCR kit (TransGen Biotech, Peking, China) on a real-time PCR

Table 1. Primer sequences used for qRT-PCR

Primer name	Sequence (5'-3')
MKRN2-F	5'-CTAACTCACATGAACCCGGAAA-3'
MKRN2-R	5'-GGCATCCAGGTAGGAATGCG-3'
GAPDH-F	5'-GAGTCAACGGATTTGGTCGTATTG-3'
GAPDH-R	5'-ATTTGCCATGGGTGGAATCATATTG-3'
CD206-F	5'-CGAGGAAGAGGTTCGGTT-3'
CD206-R	5'-ACATTTGGGTTCGGGAGT-3'
IL-10-F	5'-GAGAACCAAGACCCAGAC-3'
IL-10-R	5'-TTCACAGGGAAGAAATCG-3'
TGF-β-F	5'-TCCACGGAGAAGAACTGC-3'
TGF-β-R	5'-CAGGCTCCAAATGTAGGG-3'
ARG-1-F	5'-GCCAAGTCCAGAACCATAG-3'
ARG-1-R	5'-TCCCCATAATCCTTCACAT-3'
CD80-F	5'-GTGTTTGTTGCCTGGATT-3'
CD80-R	5'-TTGCCAGTAGATGCGAGTT-3'
CD86-F	5'-TCTGGTGCTGCTCCTCTGA-3'
CD86-R	5'-TTCCTGGTCCTGCCAAAAT-3'
TNF-α-F	5'-TCCAGGCGGTGCTTGTTC-3'
TNF-α-R	5'-TGGCAGGGGCTCTTGATG-3'
iNOS-F	5'-TGGGACCCGCACCACTAC-3'
iNOS-R	5'-CTGCCGAGATTTGAGCCT-3'

MKRN2: Makorin ring finger protein 2; GAPDH: glyceraldehyde-3-phosphate dehydrogenase; qRT-PCR: Quantitative real time polymerase chain reaction; TGF-β: Transforming growth factor-beta; TNF-α: Tumor necrosis factor-alpha; ARG-1: Arginase-1; IL: Interleukin; iNOS: Inducible nitric oxide synthase.

detection system (Thermo Fisher Scientific, USA). The reaction conditions were 95°C for 30 s, followed by 40 cycles of 95°C for 5 s and 60°C for 30 s. Relative gene expression was calculated using the $2^{-\Delta\Delta Ct}$ method, with glyceraldehyde-3-phosphate dehydrogenase (GAPDH) as the internal reference gene. The primer sequences for qRT-PCR are listed in **Table 1**.

Western blotting

Proteins were extracted using radioimmunoprecipitation assay (RIPA) buffer (89901; Thermo, USA). Equal amounts of protein were separated by 10% sodium dodecyl sulfate polyacrylamide gel electrophoresis (SDS-PAGE) and then transferred onto polyvinylidene fluoride (PVDF) membranes. After blocking with 5% non-fat milk, the membranes were incubated with the indicated primary antibodies, followed by incubation with the corresponding secondary antibodies. Protein bands were visualized suing enhanced electrochemiluminescent (ECL)_reagent (P0018M; Beyotime, Shanghai, China), and the bands were quantified using ImageJ software (National Institutes of Health, USA). Protein expression levels were normalized to β-actin and expressed as relative fold changes. All experiments were repeated three times. All primary antibodies are listed in **Table 2**.

Macrophage differentiation and coculture

THP-1 cells were cultured and treated with phorbol 12-myristate 13-acetate (PMA; 100 ng/mL; Sigma, USA) for 24 h to induce differentiation into adherent M0-like macrophages. HGC-27 cells from the Sh-NC and Sh-MKRN2 groups were seeded into the upper compartment of Transwell insert, and M0-like macrophages were cultured in the lower chambers. After 48 h of coculture, the macrophages were collected for further experiments.

Flow cytometry

Cells were fixed with 4% paraformaldehyde and permeabilized with 0.1% Triton X-100 for 5 min. The cells were stained with anti-CD206-PE (BD Pharmingen, #555954) and anti-CD86-APC (BioLegend, #374208) antibodies. Subsequently, cells were incubated with the appropriate fixation/permeabilization regents and analyzed using a flow cytometer.

Cellular immunofluorescence

Approximately 3×10^3 TAMs were fixed with 4% paraformaldehyde. Subsequently, cells were blocked in 3% BSA and incubated with the following primary antibodies: anti-CD86 (1:100, Santa Cruz) and anti-CD206 (1:100, Santa Cruz) at 4°C for 18 h. The cells were then incubated with the corresponding secondary antibodies and counterstained as appropriate. Fluorescence images were acquired using a fluorescence microscope.

mCherry-GFP-LC3 reporter assay

Stable GC cell lines expressing mCherry-GFP-LC3 were generated by lentiviral transduction. Cells were seeded at 1×10^5 cells/well, fixed with 4% paraformaldehyde for 10 min, and then permeabilized with 0.15% Triton X-100 for 10 min. Fixed cells were incubated with DAPI for 5 min, and the coverslips were washed with PBS

Table 2. Primary antibodies for Western blotting

Primary antibody	Catalog number	Dilution ratio	Source
MKRN2	ab72055	1:1,000	Abcam, Cambridge, UK
AKT	ab38449	1:5,000	Abcam, MA, USA
p-AKT	ab8933	1:5,000	Abcam, MA, USA
PI3K	60225-1-Ig	1:1,000	Proteintech, Wuhan, China
p-PI3K	# 4228S	1:1,000	CST, MA, USA
mTOR	66888-1-Ig	1:1,000	Proteintech, Wuhan, China
p-mTOR	67778-1-Ig	1:1,000	Proteintech, Wuhan, China
p62	T55546M	1:5,000	Abmart, Shanghai, China
Beclin 1	11306-1-AP	1:1,000	Proteintech, Wuhan, China
LC3	12741 T	1:1,000	CST, MA, USA
β-actin	4967	1:1,000	CST, MA, USA

MKRN2: Makorin ring finger protein 2; AKT: protein kinase B; PI3K: phosphatidylinositol 3-kinase; mTOR: mammalian target of rapamycin; LC3: light chain 3.

for three times. Fluorescence images were acquired using a confocal microscope. Red and green fluorescent puncta were then quantified to evaluate the formation of autophagosomes and autolysosomes.

Animal experiments

To assess subcutaneous tumor growth, female BALB/c nude mice aged 4-5 weeks and weighing approximately 23.6 g were obtained from the Henan Experimental Animal Center (China). The mice were acclimated for 1 week at 25°C and 60% relative humidity before experimentation. They were housed in a semi-barrier facility under constant temperature and humidity conditions and provided sterilized feed and water. The nude mice were randomly divided into two groups, with six mice per group, using a randomized block design. All animal handling, experimental procedures, and sample collection were approved by the Ethics Committee of Nanyang Second General Hospital (Approval No. ZZU-LAC20230825 [22]). Notably, MKN-45 cells with indicated transfection status (1×10^6) were injected subcutaneously into the right dorsal flank of the mice. At humane endpoints (neurological deficits, ≥20% weight loss, or marked lethargy), the mice were sacrificed by intraperitoneal injection of sodium pentobarbital (150 mg/kg). Tumor volume was measured weekly and calculated using the formula: volume = length × width^2 × 0.5. At the end of fourth week, the tumors were harvested and weighted. The maximum tumor burden allowed by the institutional Animal Ethics Committee was 5% of the animal's body weight, and all tumors in this study remained within this limit.

Immunohistochemistry (IHC)

Mice tumor tissues and human tissue specimens were sectioned and then subjected to baking, dewaxing, rehydration, and antigen retrieval. The sections were treated with a 3% hydrogen peroxide blocking solution for 30 min. After removal of excess liquid, the sections were incubated overnight with primary antibodies against MKRN2 (1:200; #bs-9379R; Bioss, Beijing, China) and Ki-67 (1:500; #GB111141; Servicebio, Wuhan, China). The next day, the sections were incubated with the corresponding secondary antibody (#G1302; Servicebio, Wuhan, China) for 1 h. Signal development was performed using 3, 3'-diaminobenzidine (DAB; Thermo Fisher), followed by hematoxylin counterstaining. After dehydration and transparency of the slices, the immunohistochemical results were interpreted under a microscope. The presence of brownish-yellow nuclear granules was considered positive. Staining intensity was scored on a four-point scale: 0, negative; 1, weak positive; 2, moderate positive; and 3, strong positive. Samples with >10% positive cells were considered positive for Ki-67 or MKRN2 expression.

Statistical analysis

Statistical analyses were performed using Graph Pad Prism 6. Data are presented as the mean ± standard deviation (SD). Comparisons

between two groups were performed using paired or unpaired *t*-tests, as appropriate. One- or two-way ANOVA was used for comparisons involving multiple groups, and repeated-measures ANOVA was used for data collected at multiple time points. A two-sided $P<0.05$ was considered statistically significant.

Results

MKRN2 expression in GC

Data from the TIMER database indicated that MKRN2 mRNA expression was significantly higher in tumor tissues than in normal tissues (**Figure 1A**). UALCAN database also showed that MKRN2 expression was significantly elevated in GC tissues (n = 415) compared to adjacent non-cancerous tissues (n = 34) (**Figure 1B**). Furthermore, Western blotting and qRT-PCR on tissue specimens confirmed pronounced upregulation of MKRN2 in GC tissues (**Figure 1C-E**). Moreover, IHC analysis also revealed significantly stronger MKRN2 staining intensity in GC tissues than in the corresponding normal tissues (**Figure 1F**, **1G**).

Correlation between MKRN2 expression and the clinical characteristics of GC

First, analysis of the UALCAN database revealed that MKRN2 expression was significantly higher in the 41-60-year and 61-80-year groups, with the highest MKRN2 expression observed in patients aged 61-80 years (**Figure 2A**). Additionally, MKRN2 expression also differed significantly between the Grade 1 and Grade 2 groups and between Grade 1 and Grade 3 groups, indicating that MKRN2 expression was higher in Grade 2 and Grade 3 tumors than in Grade 1 tumors (**Figure 2B**). In addition, MKRN2 expression was higher in tumors from patients with *H. pylori* infection (**Figure 2C**). Moreover, MKRN2 expression was also significantly higher in the N0, N1, and N3 groups (**Figure 2D**). In terms of individual cancer stages, MKRN2 expression was notably higher in patients with stage II, III, and IV tumors (**Figure 2E**).

MKRN2 expression in GC cells

MKRN2 expression was examined in four GC cell lines (AGS, MKN-7, MKN-45, and HGC-27) and the normal gastric epithelial cell line GES-1. Both the mRNA and protein levels of MKRN2 were higher in all GC cells than in GES-1 cells (**Figure 3A-C**). Among the four GC cell lines, MKRN2 expression was highest in HGC-27 cells and lowest in AGS cells. Based on these results, HGC-27 and AGS cells were selected for subsequent functional assays.

To investigate the role of MKRN2 in GC progression, MKRN2 was overexpressed in AGS cells and knocked down in HGC-27 cells. The transfection efficiency in GC cells was confirmed by qRT-PCR and Western blotting (**Figure 3D-F**). Among the sh-MKRN2 constructs, sh-MKRN2#1 was selected for subsequent functional assays, and stable cell lines were established.

MKRN2 promoted malignant behaviors in GC cells

The CCK-8 assay verified that MKRN2 knockdown significantly reduced GC cell viability (**Figure 4A**). In addition, the number of colonies was reduced after MKRN2 knockdown (**Figure 4B**). TUNEL assay and flow cytometry showed a significant increase in the proportion of apoptotic GC cells after MKRN2 knockdown (**Figure 4C**, **4D**). Additionally, wound healing and Transwell invasion assays revealed that MKRN2 knockdown significantly inhibited the migration and invasion abilities of GC cells (**Figure 4E**, **4F**).

MKRN2 regulated autophagy in GC cells

Next, our results demonstrated that MKRN2 overexpression decreased the LC3II/I ratio and Beclin-1 expression and increased p62 expression, whereas MKRN2 knockdown produced the opposite effects (**Figure 5A**). These findings suggest that MKRN2 overexpression may suppress autophagy-related activity in GC cells.

3-MA and RAPA were used to further investigate the relationship between MKRN2 and autophagy. Western blotting showed that 3-MA treatment partially reversed the autophagy-related changes induced by MKRN2 knockdown. Conversely, RAPA treatment partially counteracted the effects of MKRN2 overexpression (**Figure 5B-D**). These results suggest that MKRN2 regulates autophagy-related processes in GC cells.

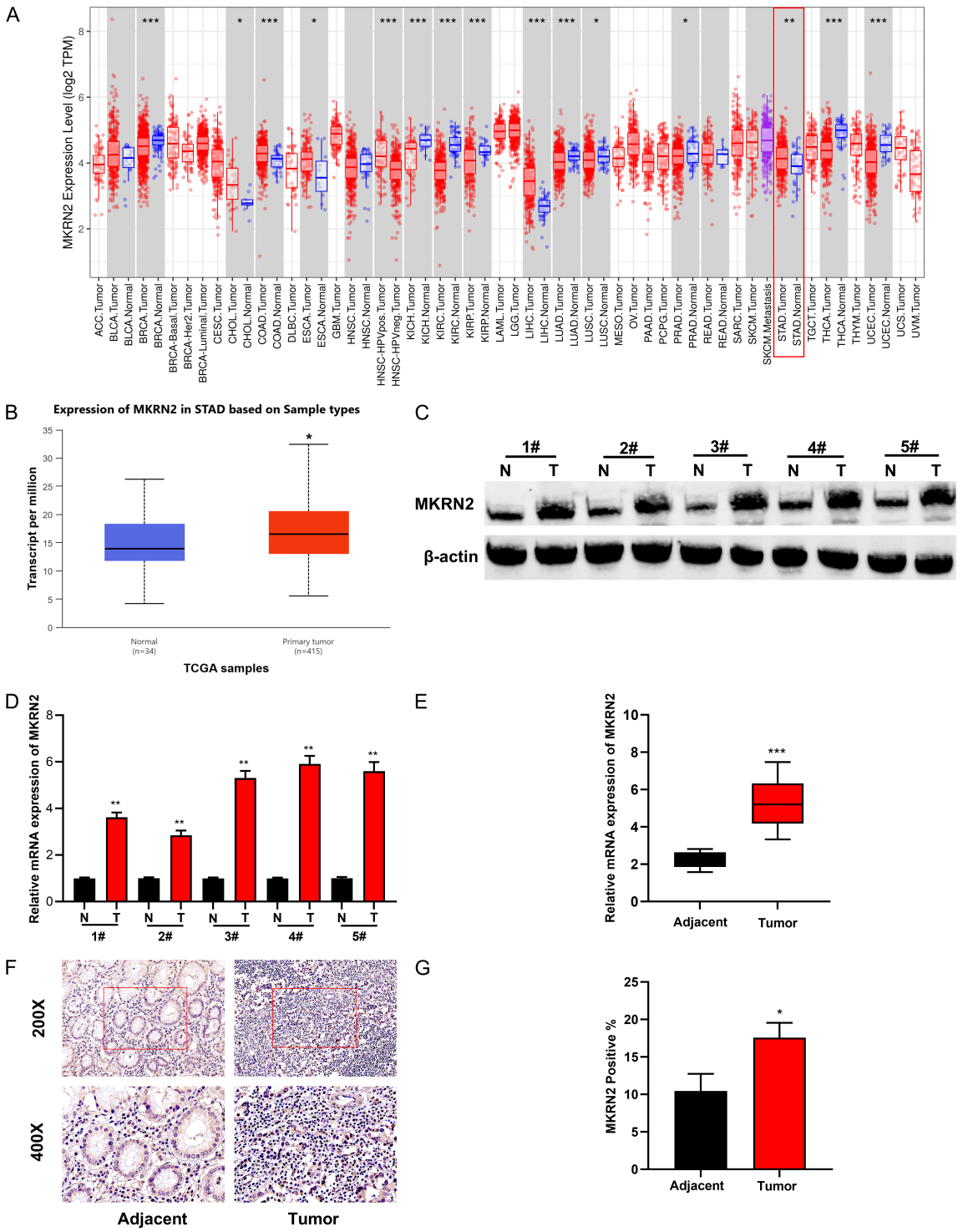


Figure 1. MKRN2 is highly expressed in GC. A. MKRN2 expression across various cancer types in the TIMER database; B. MKRN2 expression in normal (n = 34) and tumor (n = 415) tissues in the UALCAN database; C, D. MKRN2 protein expression in GC and adjacent noncancerous tissues was assessed by Western blotting; E. MKRN2 mRNA expression in GC and adjacent noncancerous tissues was assessed by qRT-PCR; F, G. Representative IHC staining of and quantitative analysis of MKRN2 expression in GC and adjacent noncancerous tissues (Scale bars: 50 μm at ×200 magnification and 20 μm at ×400 magnification). Notes: *P<0.05, **P<0.01, ***P<0.001. MKRN2: Makorin ring finger protein 2. GC: gastric cancer. TIMER: Tumor IMmune Estimation Resource. UALCAN: University of Alabama at Birmingham Cancer data analysis Portal. qRT-PCR: quantitative real-time polymerase chain reaction. IHC: Immunohistochemistry.

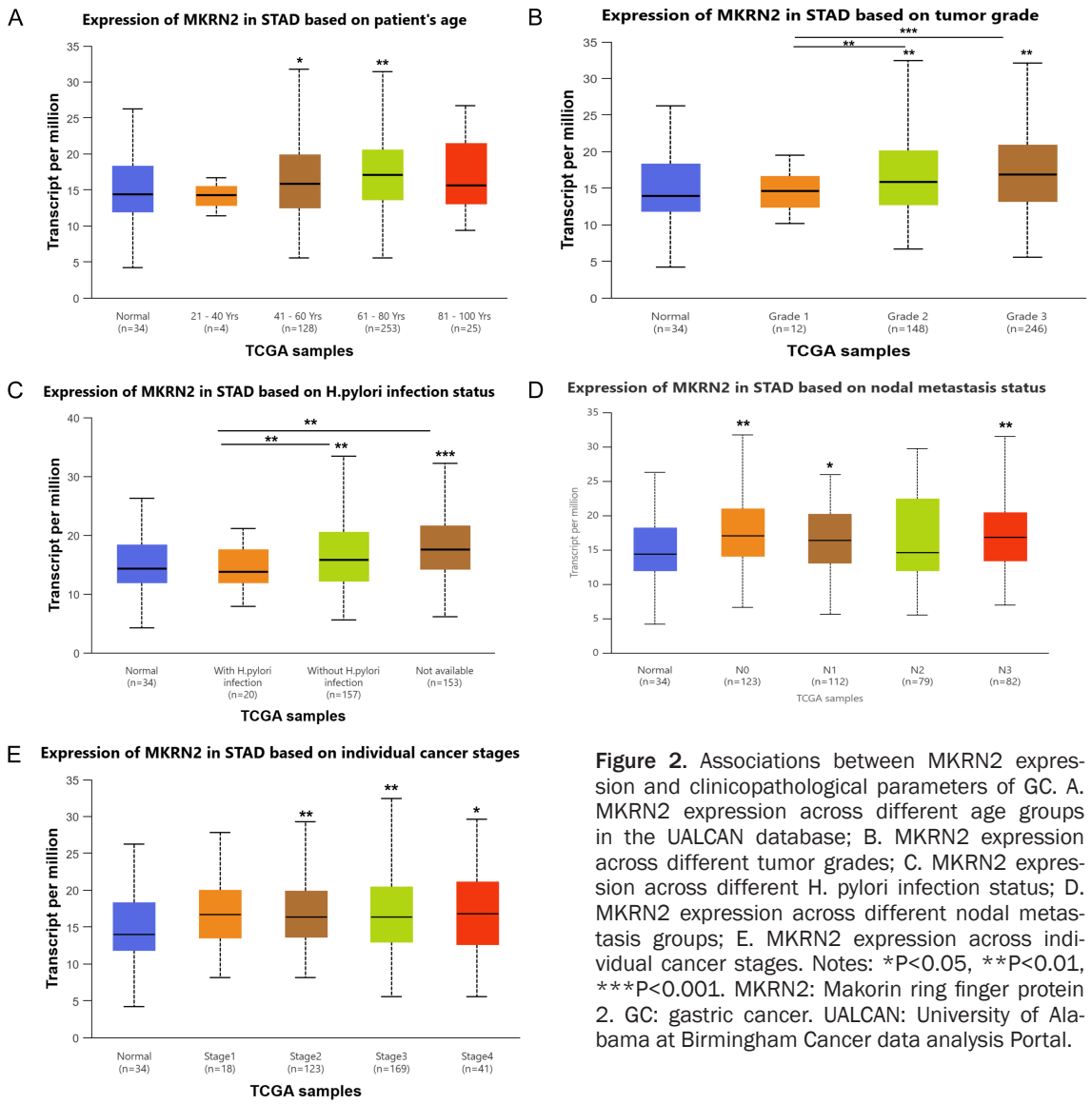


Figure 2. Associations between MKRN2 expression and clinicopathological parameters of GC. A. MKRN2 expression across different age groups in the UALCAN database; B. MKRN2 expression across different tumor grades; C. MKRN2 expression across different H. pylori infection status; D. MKRN2 expression across different nodal metastasis groups; E. MKRN2 expression across individual cancer stages. Notes: *P<0.05, **P<0.01, ***P<0.001. MKRN2: Makorin ring finger protein 2. GC: gastric cancer. UALCAN: University of Alabama at Birmingham Cancer data analysis Portal.

MKRN2 promoted the malignant behaviors of GC cells by regulating autophagy

To confirm whether MKRN2 regulates the malignant behaviors of GC cells through autophagy, RAPA was used in rescue experiments. MKRN2 overexpression enhanced cell viability and proliferation, whereas RAPA treatment partially reversed these effects in AGS cells (**Figure 6A**, **6B**). Similarly, TUNEL staining and flow cytometry showed that MKRN2 overexpression reduced GC cell apoptosis, and this effect was partially abolished by RAPA treatment (**Figure 6C**, **6D**). Moreover, overexpression of MKRN2 enhanced cell migration and invasion, whereas RAPA treatment inhibited these effects (**Figure 7A**, **7B**). These findings suggest that RAPA treatment can partially reverse the malignant phenotype induced by MKRN2 overexpression in GC cells.

MKRN2 knockdown inhibited tumor growth in mice

To further investigate the role of MKRN2 in GC, a stable MKRN2-knockdown MKN-45 cell line was established and subcutaneously implanted into nude mice. MKRN2 knockdown significantly reduced the growth of subcutaneous xenograft tumors, as reflected by decreases in tumor volume and weight (**Figure 8A-C**). IHC staining further demonstrated considerably weaker staining intensity of Ki67 and MKRN2 in xenograft tumor tissues from the sh-MKRN2

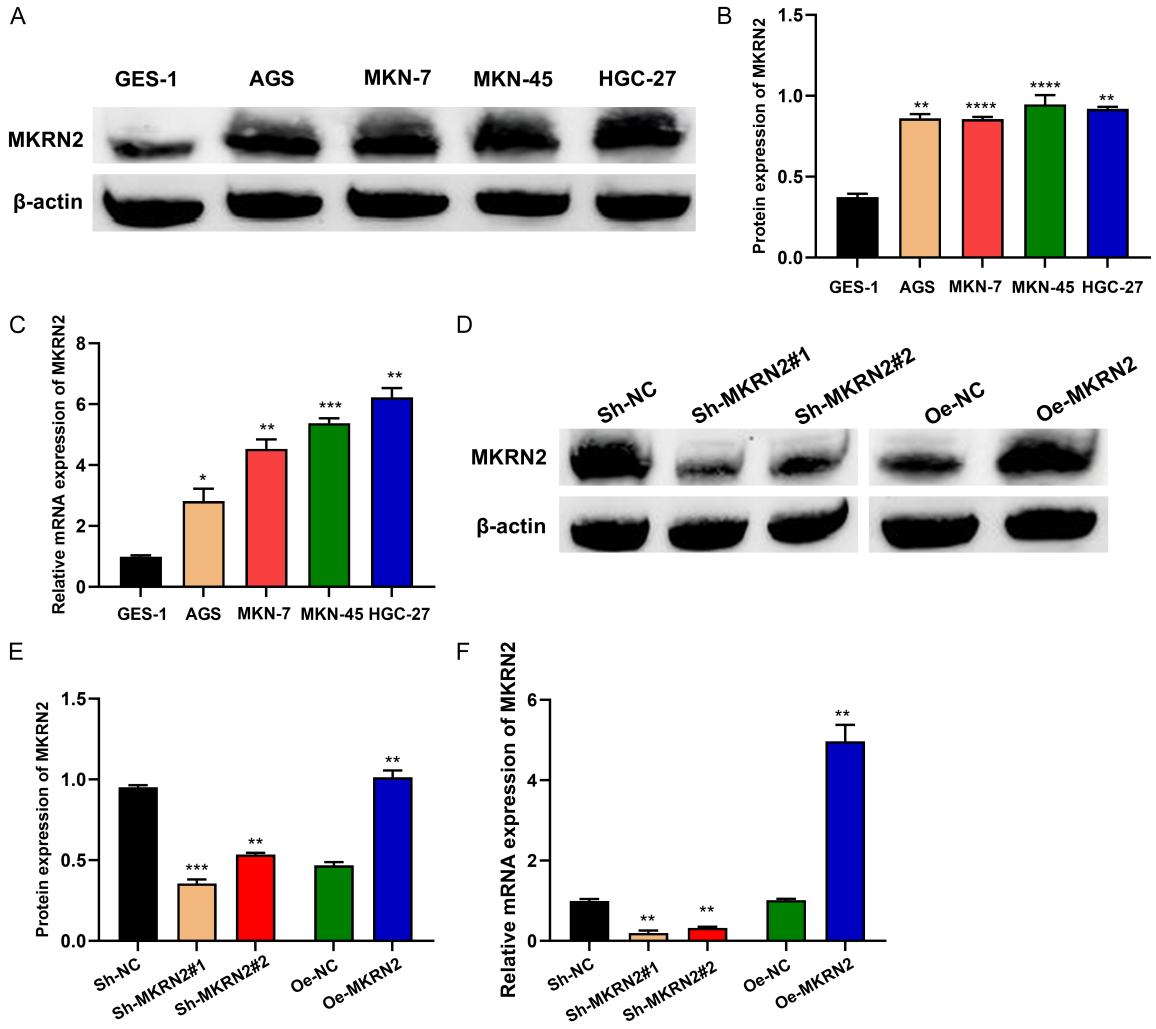


Figure 3. MKRN2 expression in GC cells. A, B. MKRN2 protein expression in GC cell lines and normal gastric epithelial cells was assessed by Western blotting; C. MKRN2 mRNA expression was assessed by qRT-PCR; D, E. MKRN2 protein expression in GC cells following the indicated transfection was assessed by Western blotting; F. MKRN2 mRNA expression of GC cells following the indicated transfections was assessed by qRT-PCR. Notes: *P<0.05, **P<0.01, ***P<0.001, ****P<0.0001. MKRN2: Makorin ring finger protein 2. GC: gastric cancer. qRT-PCR: quantitative real-time polymerase chain reaction.

group (**Figure 8D**, **8E**). Collectively, these findings indicate that MKRN2 downregulation inhibits GC growth *in vivo*.

MKRN2 regulated macrophage M2 polarization in GC

To further explore the effect of MKRN2 on macrophage M2 polarization, THP-1 cells were differentiated into M0 macrophages and cocultured with sh-NC or sh-MKRN2 GC cells. Immunofluorescence and flow cytometry showed that the expression of M2 type markers CD206 was decreased in macrophages cocultured with sh-MKRN2 GC cells, whereas CD86 expression was increased (**Figure 9A**, **9B**).

qRT-PCR was then performed to measure the mRNA levels of M1 macrophage markers (CD80, CD86, TNF-α, and iNOS) and M2 macrophage markers (CD206, IL-10, TGF-β, and ARG-1). Compared with TAMs cocultured with sh-NC GC cells, macrophages cocultured with sh-MKRN2 GC cells showed significantly increased expression of M1 macrophage markers and decreased expression of M2 macrophage markers (**Figure 9C**). Taken together, these findings suggest that, in the co-culture system, MKRN2 promotes M2-like macrophage polar-

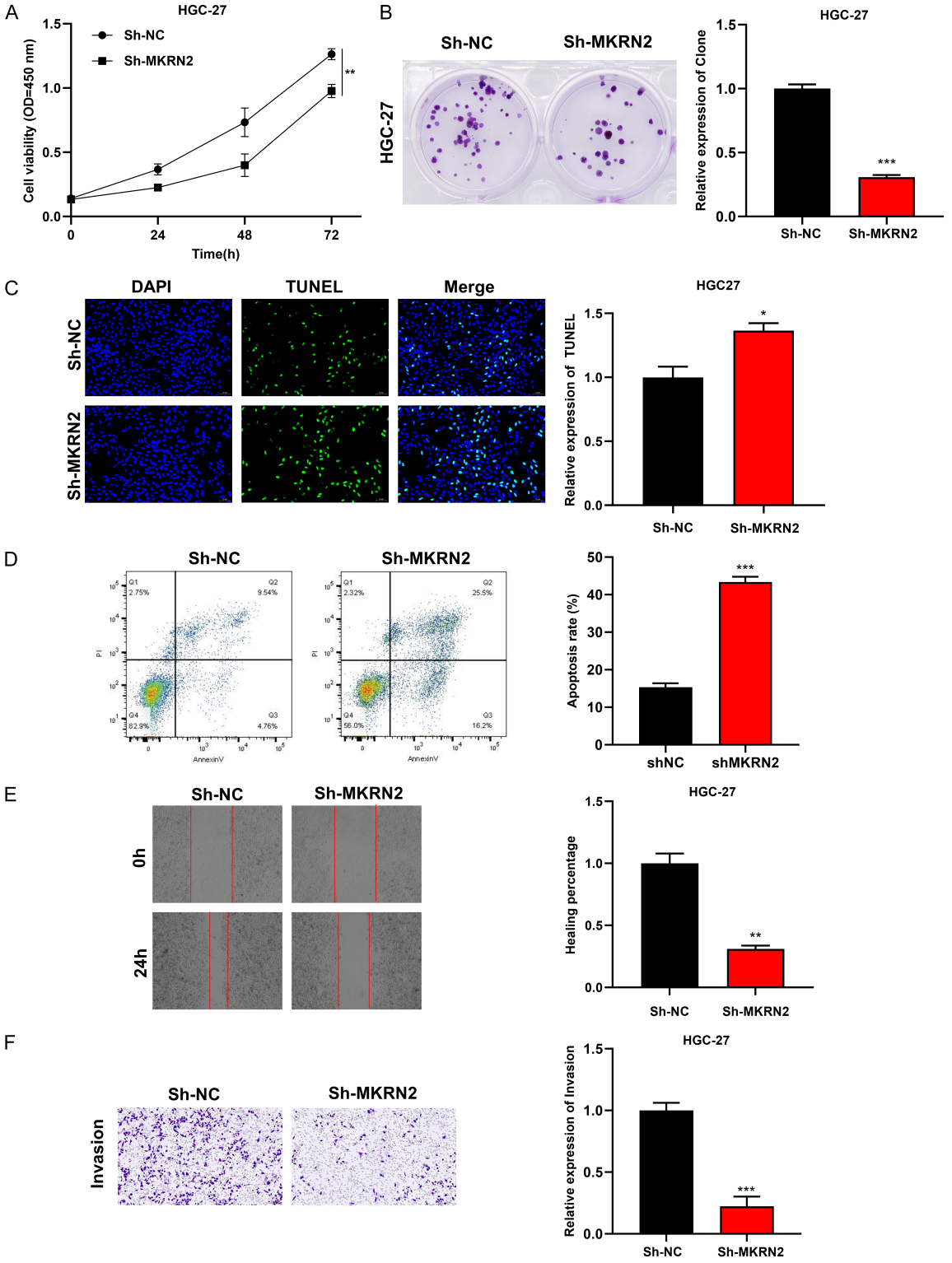


Figure 4. MKRN2 knockdown suppresses the malignant behavior of GC cells. A. Cell viability was assessed using the CCK-8 assay; B. Colony formation was assessed using the colony formation assay; C, D. Cell apoptosis was evaluated using TUNEL staining and flow cytometry (×200, scale bars = 50 μm) and flow cytometry. E, F. Cell migration and invasion were evaluated using wound-healing and Transwell invasion assays (×100, scale bars = 100 μm). Notes: *P<0.05, **P<0.01, ***P<0.001. MKRN2: Makorin ring finger protein 2. GC: gastric cancer. CCK-8: cell counting kit-8. TUNEL: terminal deoxynucleotidyl transferase dUTP nick end labeling.

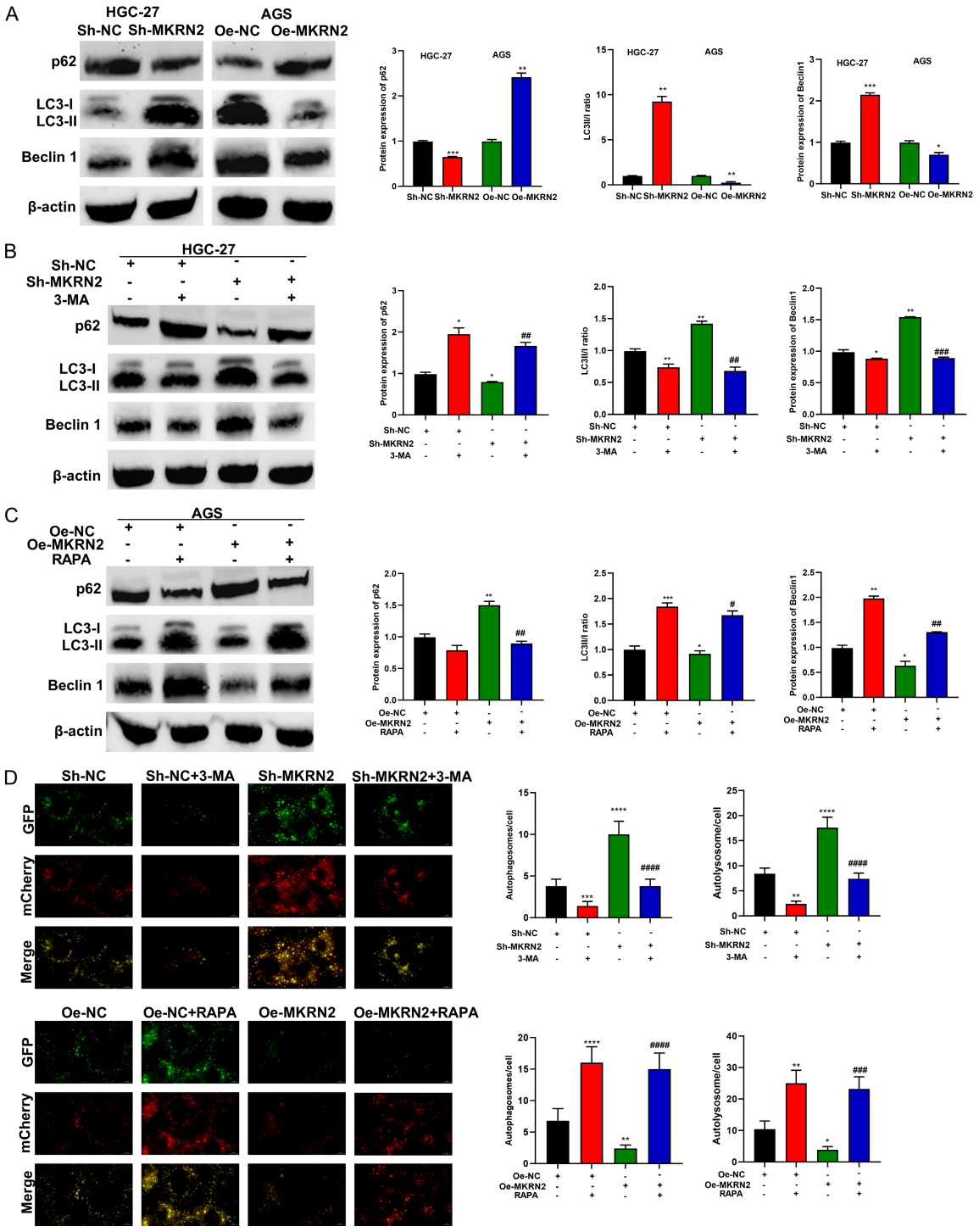


Figure 5. MKRN2 regulated autophagy-related activities in GC cells. A. Effects of MKRN2 expression on autophagy-related proteins in GC cells; B, C. After the indicated transfection, GC cells were treated with 3-MA (5 mM) or RAPA (10 ng/ml) for 12 h, and autophagy-related protein expression was assessed by western blotting; D. The distribution of GFP-mCherry-LC3B in GC cells was examined by fluorescence microscopy (×600, scale bars = 20 μm). Merged yellow puncta represent autophagosomes, whereas red-only puncta represent autolysosomes. The number of yellow and red puncta were quantified to evaluate autophagic flux. Notes: *P<0.05, **P<0.01, ***P<0.001, ****P<0.0001 compared with the control group. #P<0.05, ##P<0.01, ###P<0.001, ####P<0.0001 compared with the Sh-MKRN2 or Oe-MKRN2 group. MKRN2: Makorin ring finger protein 2. GC: gastric cancer. 3-MA: 3-methyladenine. RAPA: rapamycin.

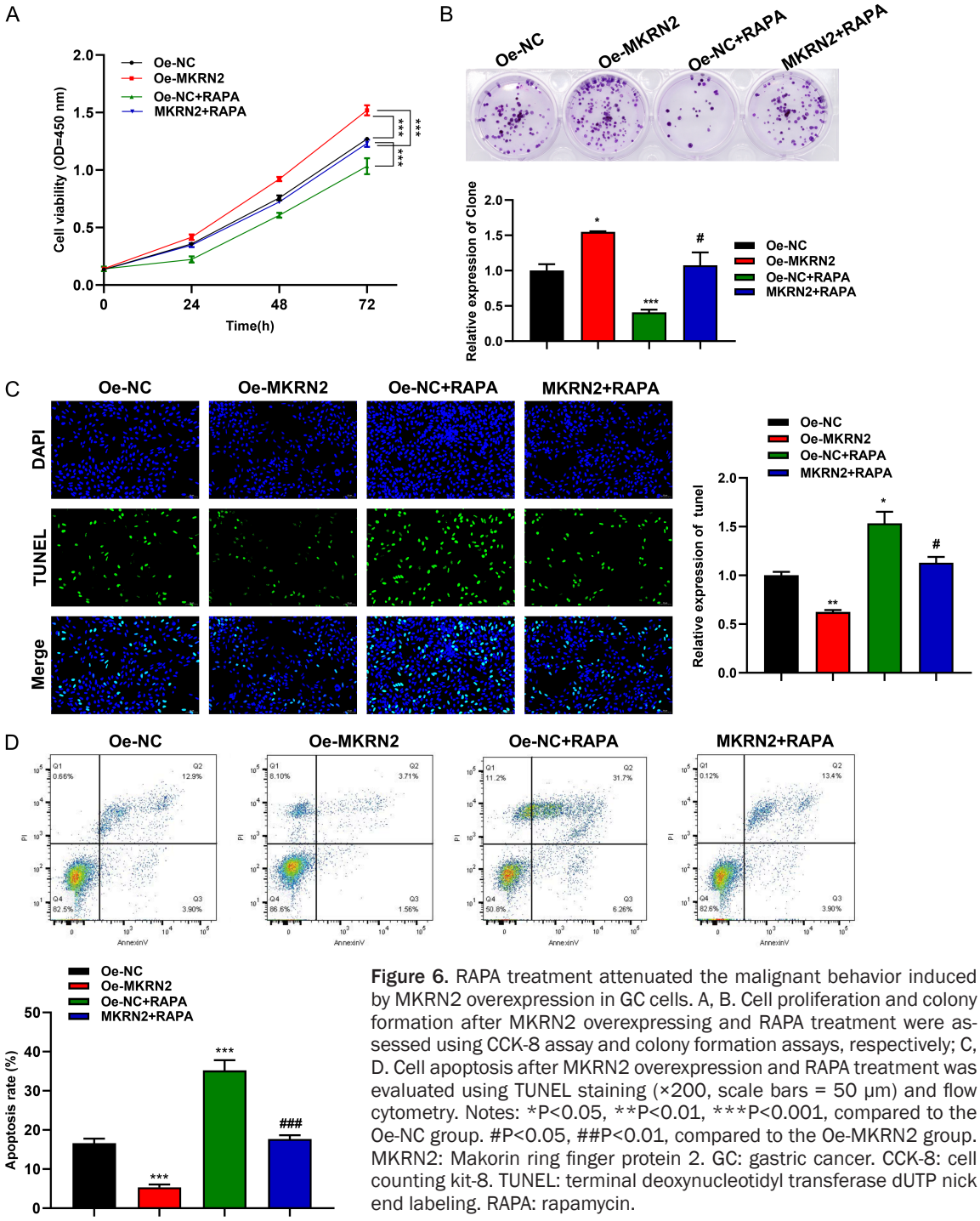


Figure 6. RAPA treatment attenuated the malignant behavior induced by MKRN2 overexpression in GC cells. A, B. Cell proliferation and colony formation after MKRN2 overexpressing and RAPA treatment were assessed using CCK-8 assay and colony formation assays, respectively; C, D. Cell apoptosis after MKRN2 overexpression and RAPA treatment was evaluated using TUNEL staining (×200, scale bars = 50 μm) and flow cytometry. Notes: *P<0.05, **P<0.01, ***P<0.001, compared to the Oe-NC group. #P<0.05, ##P<0.01, compared to the Oe-MKRN2 group. MKRN2: Makorin ring finger protein 2. GC: gastric cancer. CCK-8: cell counting kit-8. TUNEL: terminal deoxynucleotidyl transferase dUTP nick end labeling. RAPA: rapamycin.

ization and suppresses M1-like macrophage polarization in GC.

Effects of MKRN2 on the PI3K/Akt/mTOR signaling pathway

The PI3K/Akt/mTOR signaling pathway is closely associated with autophagy and the development of various tumors [23, 24]. MKRN2 knockdown decreased the levels of phosphorylated PI3K, Akt, and mTOR, while the levels of total PI3K, Akt, and mTOR remained largely unchanged in sh-MKRN2-transfected GC cells (**Figure 10A**, **10B**). Conversely, MKRN2 overexpression exerted an opposite effects. Rescue experiments were then performed to further

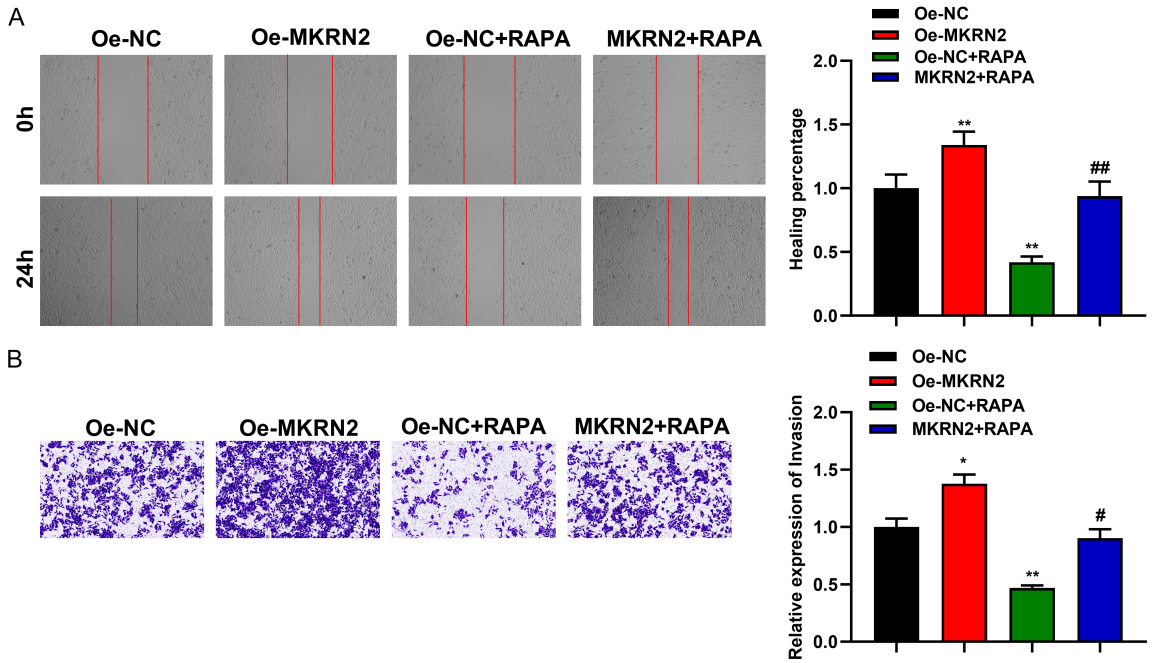


Figure 7. RAPA treatment attenuated GC cell malignant behavior induced by MKRN2 overexpression. A, B. Cell migration and invasion following MKRN2 overexpression and RAPA treatment were evaluated using wound-healing and Transwell invasion assays, respectively (×100, scale bars = 100 μm). Notes: *P<0.05, **P<0.01, ***P<0.001, compared to the Oe-NC group. #P<0.05, ##P<0.01, compared to the Oe-MKRN2 group. MKRN2: Makorin ring finger protein 2. GC: gastric cancer. CCK-8: cell counting kit-8. TUNEL: terminal deoxynucleotidyl transferase dUTP nick end labeling. RAPA: rapamycin.

determined whether MKRN2 regulates GC pathogenesis via this pathway. Treatment with LY294002, a PI3K/Akt/mTOR pathway inhibitor, partially reversed the effects induced by MKRN2 overexpression (**Figure 10C**, **10D**). Therefore, these findings suggest that MKRN2 may regulate GC progression, at least in part, through the PI3K/Akt/mTOR pathway.

Discussion

As one of the most prevalent malignancies worldwide, the incidence and mortality rates of GC continue to rise, especially in East Asia [25]. This high disease burden may be associated with multiple factors, including dietary habits, genetic susceptibility, and pathogen infection. Although diagnostic and therapeutic techniques have been improved, the overall prognosis of GC patients remains unsatisfactory. With the continuous exploration of tumor-related genes, gene-targeted therapy has gradually become a hot spot in tumor research, providing new ideas for the diagnosis and treatment of GC [26-28]. In this study, we investigated the tumor-promoting role of MKRN2 in GC. Our results showed that MKRN2 was significantly upregulated in GC tissues and cells promoted GC progression. More importantly, MKRN2 deficiency reduced the phosphorylation levels of PI3K/Akt/mTOR pathway.

The role of MKRN2 in tumorigenesis is complex and exhibits outstanding tissue-specific duality, with MKRN2 functioning as either an oncogene or a tumor suppressor depending on the cellular context. MKRN2 acts as a suppressor in various cancers, including non-small cell lung cancer [14], ovarian cancer [29], colorectal cancer [30], and renal cell carcinoma [17]. In contrast, MKRN2 may also function as an oncogene that promotes tumor initiation and progression. In hepatocellular carcinoma, MKRN2 is upregulated and correlated with cell cycle and proliferation of tumor cells [16]. Furthermore, elevated MKRN2 expression promotes melanoma cell proliferation in a p53-dependent manner, supporting its carcinogenic role [31]. Contrary to previous findings [19], our data demonstrated that MKRN2 was upregulated in GC tissues and cells. Mechanistically, MKRN2 knockdown inhibited GC cell viability,

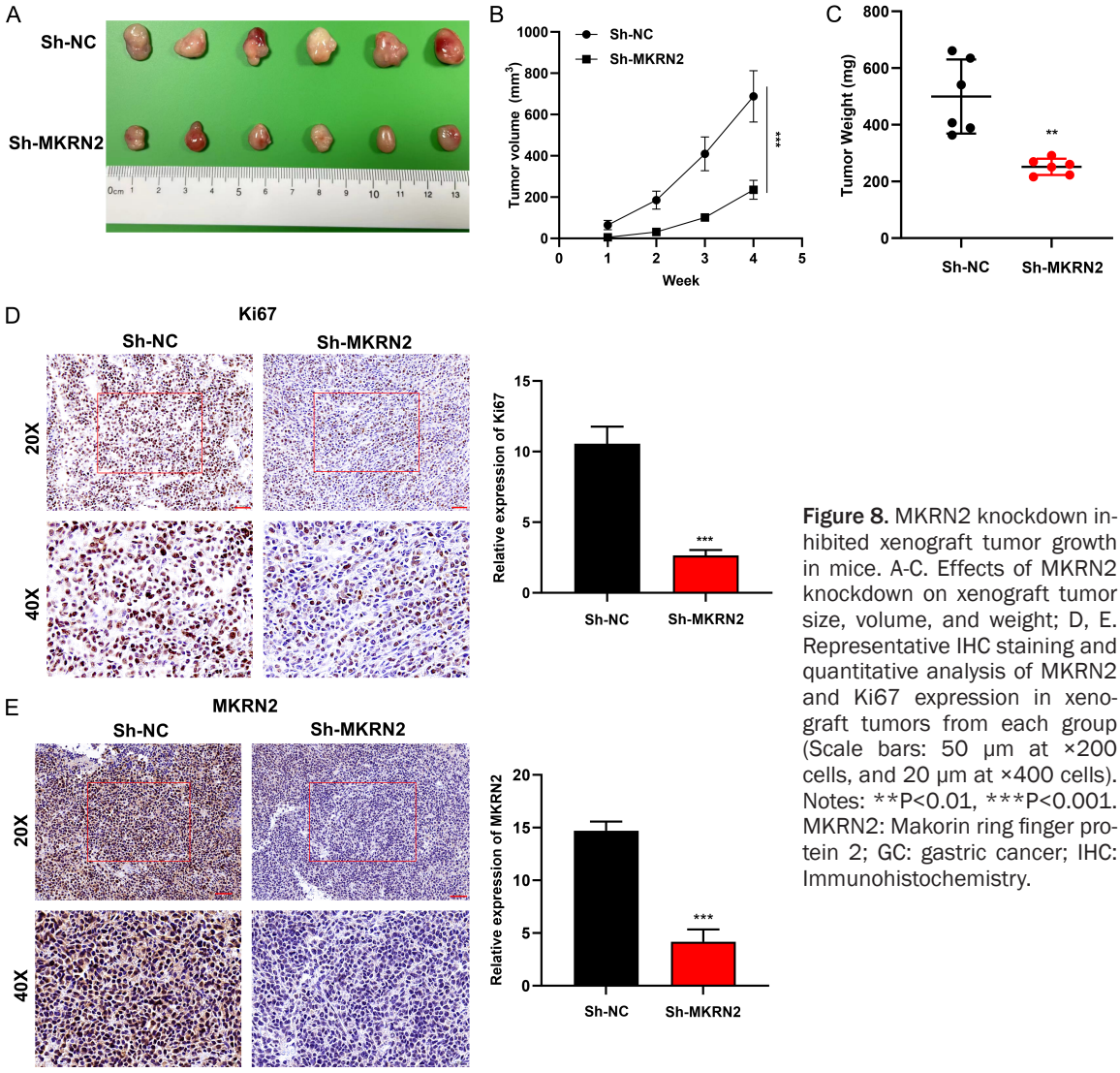


Figure 8. MKRN2 knockdown inhibited xenograft tumor growth in mice. A-C. Effects of MKRN2 knockdown on xenograft tumor size, volume, and weight; D, E. Representative IHC staining and quantitative analysis of MKRN2 and Ki67 expression in xenograft tumors from each group (Scale bars: 50 μm at ×200 cells, and 20 μm at ×400 cells). Notes: **P<0.01, ***P<0.001. MKRN2: Makorin ring finger protein 2; GC: gastric cancer; IHC: Immunohistochemistry.

proliferation, migration, and invasion and promoted apoptosis, whereas MKRN2 overexpression produced the opposite effects. Moreover, mice bearing xenograft derived from sh-MKRN2-transfected cells exhibited reduced tumor weight and volume. These findings support an oncogenic role for MKRN2 in GC progression.

Autophagy is a highly conserved cellular process that maintains cellular homeostasis by degrading and recycling damaged organelles, misfolded proteins, and intracellular pathogens [32, 33]. Nevertheless, autophagy dysregulation has been implicated in the pathogenesis of numerous diseases, including cancer [34]. Our findings revealed that MKRN2 overexpression decreased the LC3II/I ratio and Beclin1 expression and increased p62 expression, whereas MKRN2 knockdown produced an opposite effect. Interestingly, treatment with 3-MA partially reversed the effects of MKRN2 knockdown on autophagy marker proteins in GC cells, whereas RAPA partially reversed the suppression of autophagy-related activity induced by MKRN2 overexpression. Furthermore, we observed that RAPA treatment attenuated the enhanced malignant behavior of GC cells caused by MKRN2 overexpression. These findings suggest that MKRN2 may promote GC progression, at least in part, by suppressing autophagy-related processes.

TAMs are an important innate immune cell population in TME and involved in angiogenesis, chronic inflammation, tumor-cell invasion and

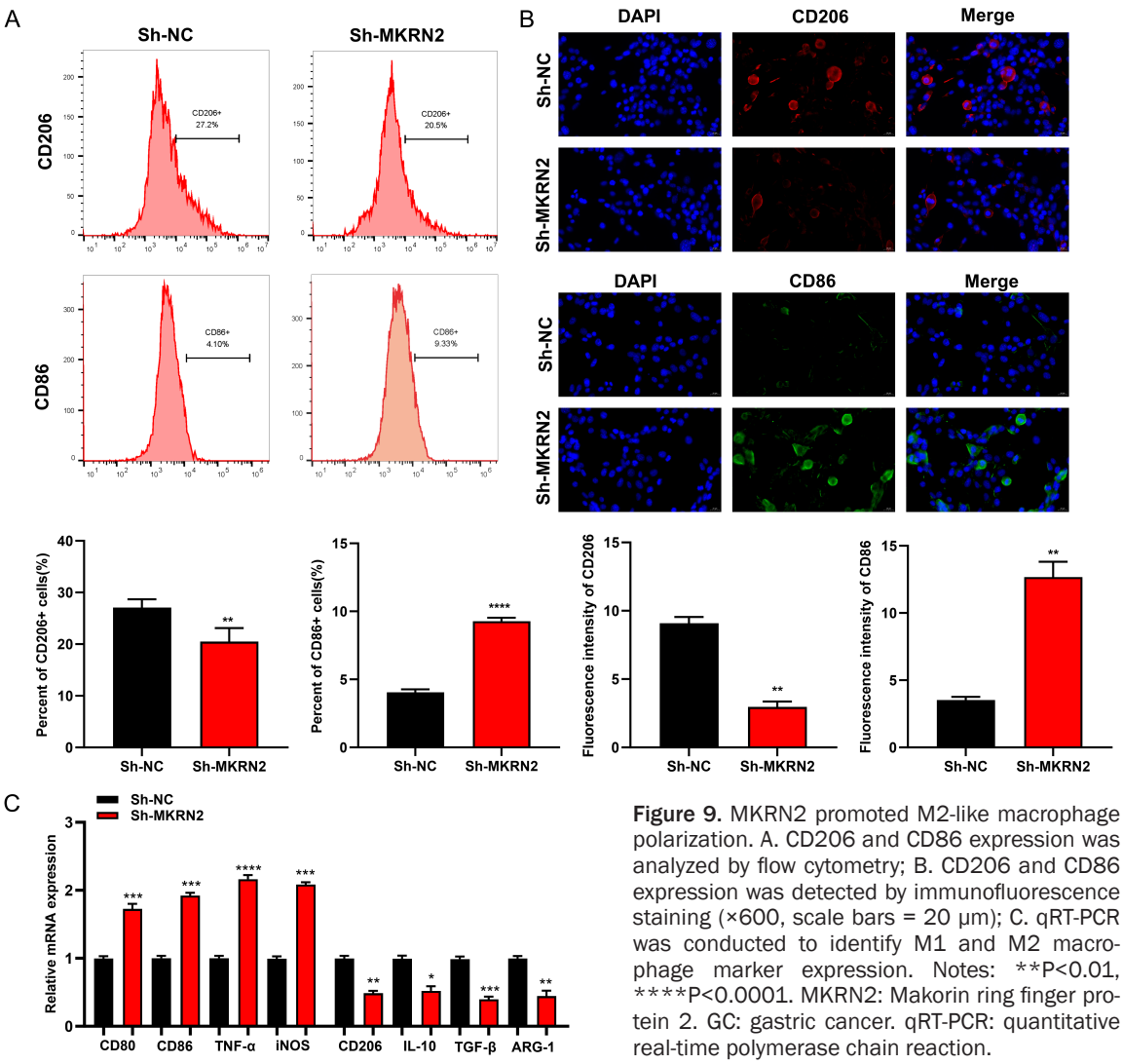


Figure 9. MKRN2 promoted M2-like macrophage polarization. A. CD206 and CD86 expression was analyzed by flow cytometry; B. CD206 and CD86 expression was detected by immunofluorescence staining (×600, scale bars = 20 μm); C. qRT-PCR was conducted to identify M1 and M2 macrophage marker expression. Notes: **P<0.01, ****P<0.0001. MKRN2: Makorin ring finger protein 2. GC: gastric cancer. qRT-PCR: quantitative real-time polymerase chain reaction.

metastasis, and immune escape [35]. An increased abundance of TAMs has been positively correlated with greater invasiveness, metastasis, and poorer prognosis in patients with GC [36, 37]. Therefore, we further investigated the effect of MKRN2 on M2 macrophage polarization. In our coculture systems, MKRN2 knockdown in GC cells inhibited M2-like polarization and promoted M1-like polarization.

Aberrant activation or dysfunction of the PI3K/Akt/mTOR signaling pathway has been associated with approximately 50% of malignant tumors, making it one of the most frequently dysregulated pathways in human cancers [38]. Recent studies have shown that transmembrane protein 65 (TMEM65) promotes GC progression by activating the PI3K/Akt/mTOR pathway [39]. Su et al. reported that interactions between TAMs and GC cells promoted chemotherapy resistance through the C-X-C motif chemokine ligand 5 (CXCL5)/PI3K/Akt/mTOR pathway [40]. In the present study, MKRN2 knockdown decreased the levels of p-PI3K, p-Akt, and p-mTOR. Subsequent experiments revealed that LY294002 treatment partially reversed the increases in PI3K, Akt, and mTOR phosphorylation induced by MKRN2 overexpression. Therefore, MKRN2 may regulate autophagy in GC cells through the PI3K/Akt/mTOR signaling pathway. Nevertheless, further functional rescue experiments are required to confirm the role of this pathway. The identification of direct substrates of MKRN2 and the specific E3 ubiquitin ligase-dependent mechanism remain to be elucidated. Future

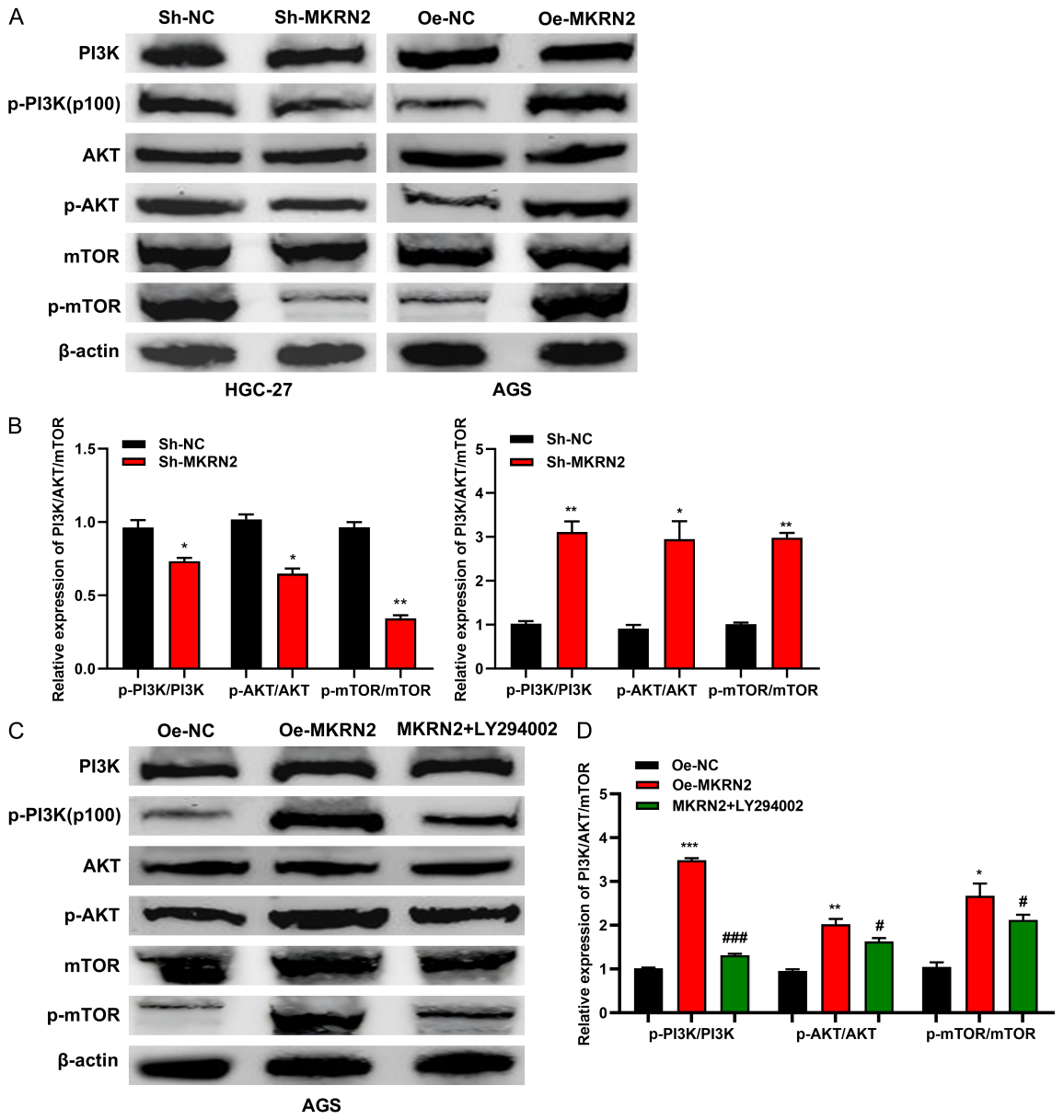


Figure 10. MKRN2 activated the PI3K/Akt/mTOR pathway in GC cells. A, B. Western blot analysis was performed to assess the effects of MKRN2 expression on PI3K/Akt/mTOR pathway-related proteins in GC cells; C, D. LY294002 reversed the increases in pathway-related protein phosphorylation induced MKRN2 overexpression. Notes: *P<0.05, **P<0.01, ***P<0.001, compared to the Oe-NC group. #P<0.05, ###P<0.001, compared to the Oe-MKRN2 group. MKRN2: Makorin ring finger protein 2. GC: gastric cancer. PI3K/Akt/mTOR: phosphatidylinositol 3-kinase/protein kinase B/mammalian target of rapamycin.

studies with larger clinical cohorts should also investigate the associations of MKRN2 expression with pathological characteristics and survival outcomes in GC patients. Finally, although our in vitro studies provide mechanistic insights into macrophage-tumor interactions, they do not fully recapitulate the complex TME in vivo. Studies utilizing immunocompetent or humanized mouse models are required to validate these findings under more physiologically relevant conditions.

Conclusion

In this study, MKRN2 was upregulated in GC and promoted malignant progression of GC cells, potentially by suppressing autophagy through the PI3K/Akt/mTOR signaling pathway.

Therefore, MKRN2 may represent a potential therapeutic target for GC.

Acknowledgements

This work was supported by grant LHGJ2021-0974 as a joint construction project.

Written informed consent was obtained from all participants prior to inclusion in the study.

Disclosure of conflict of interest

None.

Address correspondence to: Miao Wang, Department of Oncology, Nanyang Second General Hospital, No. 66 Jianshe East Road, Nanyang 473000, Henan, China. E-mail: 15237758355@163.com

References

[1] Bray F, Laversanne M, Sung H, Ferlay J, Siegel RL, Soerjomataram I and Jemal A. Global cancer statistics 2022: GLOBOCAN estimates of incidence and mortality worldwide for 36 cancers in 185 countries. CA Cancer J Clin 2024; 74: 229-263.

[2] Luo D, Liu Y, Lu Z and Huang L. Targeted therapy and immunotherapy for gastric cancer: rational strategies, novel advancements, challenges, and future perspectives. Mol Med 2025; 31: 52.

[3] Guan WL, He Y and Xu RH. Gastric cancer treatment: recent progress and future perspectives. J Hematol Oncol 2023; 16: 57.

[4] Conti CB, Agnesi S, Scaravaglio M, Masseria P, Dinelli ME, Oldani M and Uggeri F. Early gastric cancer: update on prevention, diagnosis and treatment. Int J Environ Res Public Health 2023; 20: 2149.

[5] Chen Y, Jia K, Xie Y, Yuan J, Liu D, Jiang L, Peng H, Zhong J, Li J, Zhang X and Shen L. The current landscape of gastric cancer and gastroesophageal junction cancer diagnosis and treatment in China: a comprehensive nationwide cohort analysis. J Hematol Oncol 2025; 18: 42.

[6] Zhang M, Zhong J, Song Z, Xu Q, Chen Y and Zhang Z. Regulatory mechanisms and potential therapeutic targets in precancerous lesions of gastric cancer: a comprehensive review. Biomed Pharmacother 2024; 177: 117068.

[7] Wang T, Liu W, Wang C, Ma X, Akhtar MF, Li Y and Li L. MRKNs: gene, functions, and role in disease and infection. Front Oncol 2022; 12: 862206.

[8] Gray TA, Azama K, Whitmore K, Min A, Abe S and Nicholls RD. Phylogenetic conservation of the makorin-2 gene, encoding a multiple zinc-finger protein, antisense to the RAF1 proto-oncogene. Genomics 2001; 77: 119-126.

[9] Guseva EA, Emelianova MA, Sidorova VN, Tyulpakov AN, Dontsova OA and Sergiev PV. Diversity of molecular functions of RNA-binding ubiquitin ligases from the MKRN protein family. Biochemistry (Mosc) 2024; 89: 1558-1572.

[10] Shin C, Ito Y, Ichikawa S, Tokunaga M, Sakata-Sogawa K and Tanaka T. MKRN2 is a novel ubiquitin E3 ligase for the p65 subunit of NF-kappaB and negatively regulates inflammatory responses. Sci Rep 2017; 7: 46097.

[11] Wang J, Wang X, Chen F, Ning Q, Liu Y, Zhu Y, Wei W, Leng M, Wang Z, Jin P and Li Q. N6-methyladenosine modification of lncCCKAR-5 regulates autophagy in human umbilical cord mesenchymal stem cells by destabilizing LMNA and inhibits diabetic wound healing. J Invest Dermatol 2024; 144: 1148-1160, e15.

[12] Wang L, Yong YL, Wang KK, Xie YX, Qian YC, Zhou FM, Qiu JG and Jiang BH. MKRN2 knockout causes male infertility through decreasing STAT1, SIX4, and TNC expression. Front Endocrinol (Lausanne) 2023; 14: 1138096.

[13] Qiu JG, Sang P, Zhou FM, Zhang XQ, Wang W, Qian YC, Zhang Y, Wang L, Liu LZ, Xue YQ, Zhao X, Shan Q, Huang P, Zheng SG and Jiang BH. Novel role of MKRN2 in regulating tumor growth through host microenvironment and macrophage M1 to M2 switch. Cancer Lett 2025; 633: 218035.

[14] Jiang J, Xu Y, Ren H, Wudu M, Wang Q, Song X, Su H, Jiang X, Jiang L and Qiu X. MKRN2 inhibits its migration and invasion of non-small-cell lung cancer by negatively regulating the PI3K/Akt pathway. J Exp Clin Cancer Res 2018; 37: 189.

[15] Pan Y, Hua S, Yang R, He Q, Xu Y, Jiang Z, Gong X, Zhang S, Wang X, Yu H, Wu H, Wen H, Wang P, Hang B and Wang X. A covalent molecular glue hijacks the E3 ligase MKRN2 to degrade the ribosomal protein RPS7 and induce synthetic lethality in p53-deficient NSCLC cells. Br J Pharmacol 2026; [Epub ahead of print].

[16] Chen X, Yan Z, Du X, Zhang Z, Liu X, Zhang J, Hu L, He K, Wang J and Han Y. MKRN2 enhances hepatocellular carcinoma proliferation through the p38 MAPK pathway. Hum Cell 2026; 39: 47.

[17] Yu T, Li W, Meng X, Yuan H, Ruan H, Xiao W and Zhang X. E3 ligase MKRN2 destabilizes PPP2CA proteins to inactivate canonical Wnt pathway and mitigates tumorigenesis of clear cell renal cell carcinoma. Int J Biol Sci 2025; 21: 5361-5377.

[18] Jia C, Tang H, Yang Y, Yuan S, Han T, Fang M, Huang S, Hu R, Li C and Geng W. Ubiquitination of IGF2BP3 by E3 ligase MKRN2 regulates the proliferation and migration of human neuro-

blastoma SHSY5Y cells. Biochem Biophys Res Commun 2020; 529: 43-50.
[19] Liu Z, Xiang S, Guo X, Zhou J, Liao L, Kou J and Zhang J. MKRN2 inhibits the proliferation of gastric cancer by downregulating PKM2. Aging (Albany NY) 2022; 14: 2004-2013.
[20] Lei X, Lei Y, Li JK, Du WX, Li RG, Yang J, Li J, Li F and Tan HB. Immune cells within the tumor microenvironment: biological functions and roles in cancer immunotherapy. Cancer Lett 2020; 470: 126-133.
[21] Toledo B, Zhu Chen L, Paniagua-Sancho M, Marchal JA, Perán M and Giovannetti E. Deciphering the performance of macrophages in tumour microenvironment: a call for precision immunotherapy. J Hematol Oncol 2024; 17: 44.
[22] Christofides A, Strauss L, Yeo A, Cao C, Charest A and Boussiotis VA. The complex role of tumor-infiltrating macrophages. Nat Immunol 2022; 23: 1148-1156.
[23] Xu Z, Han X, Ou D, Liu T, Li Z, Jiang G, Liu J and Zhang J. Targeting PI3K/AKT/mTOR-mediated autophagy for tumor therapy. Appl Microbiol Biotechnol 2020; 104: 575-587.
[24] Jiang M, Zhang K, Zhang Z, Zeng X, Huang Z, Qin P, Xie Z, Cai X, Ashrafizadeh M, Tian Y and Wei R. PI3K/AKT/mTOR axis in cancer: from pathogenesis to treatment. MedComm (2020) 2025; 6: e70295.
[25] Xie T, Zhang Z, Peng Z and Shen L. Next stage of collaboration in East Asia gastric cancer treatment. Chin Clin Oncol 2023; 12: 39.
[26] Shi T, Zhang Y, Wang Y, Song X, Wang H, Zhou X, Liang K, Luo Y, Che K, Wang X, Pan Y, Liu F, Yang J, Liu Q, Yu L, Liu B and Wei J. DKK1 promotes tumor immune evasion and impedes Anti-PD-1 treatment by inducing immunosuppressive macrophages in gastric cancer. Cancer Immunol Res 2022; 10: 1506-1524.
[27] Xu Y, Zhang C, Wu J, Qiu M, Zhu M, Wang C and Feng Y. Integrating single-cell RNA sequencing and spatial transcriptomics to reveal the glycolysis-related gene GPRC5A as a potential biomarker for gastric cancer by machine learning. Int J Biol Macromol 2025; 323: 147059.
[28] Li Y, Chen M, Chen Q, Yuan M, Zeng X, Zeng Y, He M, Wang B and Han B. Bioinformatics identification of therapeutic gene targets for gastric cancer. Adv Ther 2023; 40: 1456-1473.
[29] Jiang FZ, Xia QJ, Wu L and Zhang YM. Overexpression of MKRN2 inhibits the growth of ovarian cancer cells. Mol Biol (Mosk) 2023; 57: 687-688.
[30] Qi P, Yexie Z, Xue C, Huang G, Zhao Z and Zhang X. LINC00294/miR-620/MKRN2 axis provides biomarkers and negatively regulates malignant progression in colorectal carcinoma. Hum Exp Toxicol 2023; 42: 960327123-1167577.
[31] Zhang Y, Cui N and Zheng G. Ubiquitination of P53 by E3 ligase MKRN2 promotes melanoma cell proliferation. Oncol Lett 2020; 19: 1975-1984.
[32] Li X, He S and Ma B. Autophagy and autophagy-related proteins in cancer. Mol Cancer 2020; 19: 12.
[33] Niu X, You Q, Hou K, Tian Y, Wei P, Zhu Y, Gao B, Ashrafizadeh M, Aref AR, Kalbasi A, Cañadas I, Sethi G, Tergaonkar V, Wang L, Lin Y, Kang D and Klionsky DJ. Autophagy in cancer development, immune evasion, and drug resistance. Drug Resist Updat 2025; 78: 101170.
[34] Liu J, Wu Y, Meng S, Xu P, Li S, Li Y, Hu X, Ouyang L and Wang G. Selective autophagy in cancer: mechanisms, therapeutic implications, and future perspectives. Mol Cancer 2024; 23: 22.
[35] de Visser KE and Joyce JA. The evolving tumor microenvironment: from cancer initiation to metastatic outgrowth. Cancer Cell 2023; 41: 374-403.
[36] Zhang Z, Yu K, Cao Y, Xie P, Wang L, Shen Z and Qin J. TREM2 facilitates gastric cancer progression and immune evasion via inhibiting TRIM21-mediated STAT1 degradation in tumor-associated macrophages. Cell Death Dis 2025; 16: 845.
[37] Li J, Sun J, Zeng Z, Liu Z, Ma M, Zheng Z, He Y and Kang W. Tumour-associated macrophages in gastric cancer: from function and mechanism to application. Clin Transl Med 2023; 13: e1386.
[38] Glaviano A, Foo ASC, Lam HY, Yap KCH, Jacot W, Jones RH, Eng H, Nair MG, Makvandi P, Geoerger B, Kulke MH, Baird RD, Prabhu JS, Carbone D, Pecoraro C, Teh DBL, Sethi G, Cavalieri V, Lin KH, Javidi-Sharifi NR, Toska E, Davids MS, Brown JR, Diana P, Stebbing J, Fruman DA and Kumar AP. PI3K/AKT/mTOR signaling transduction pathway and targeted therapies in cancer. Mol Cancer 2023; 22: 138.
[39] Shi L, Wang X, Guo S, Gou H, Shang H, Jiang X, Wei C, Wang J, Li C, Wang L, Zhao Z, Yu W and Yu J. TMEM65 promotes gastric tumorigenesis by targeting YWHAZ to activate PI3K-Akt-mTOR pathway and is a therapeutic target. Oncogene 2024; 43: 931-943.
[40] Su P, Jiang L, Zhang Y, Yu T, Kang W, Liu Y and Yu J. Crosstalk between tumor-associated macrophages and tumor cells promotes chemoresistance via CXCL5/PI3K/AKT/mTOR pathway in gastric cancer. Cancer Cell Int 2022; 22: 290.